

Automatic centerline extraction of left coronary artery from X-ray rotational angiographic images

Gerardo Chacón^{a,b}, Johel Rodríguez^a, Valmore Bermúdez^a, Miguel Vera^{c,d}, Delia Madriz^e, and Antonio Bravo^e

^aGrupo de Investigación Altos Estudios de Frontera, Universidad Simón Bolívar, Cúcuta 540004, Colombia

^bGrupo de Automatización y Control, Universidad de Pamplona, Cúcuta 540004 Colombia

^cGrupo de Investigación en Ciencias Exactas, Físicas y Naturales Aplicadas, Facultad de Ciencias Básicas y Biomédicas, Universidad Simón Bolívar, Cúcuta 540004, Colombia.

^dGrupo de Investigación en Procesamiento Computacional de Datos, Universidad de Los Andes-Táchira, San Cristóbal 5001, Venezuela.

^ePrograma Calidad y Productividad Organizacional, Decanato de Investigación, Universidad Nacional Experimental del Táchira, San Cristóbal 5001, Venezuela.

ABSTRACT

Rotational X-ray coronary angiography is a medical imaging technique safe and effective in identifying of the luminal disease, which considers a significant reduction in radiation exposure and contrast medium volume compared to conventional angiography. The main objective of this research is to propose a computational approach to automatically extract a description of the morphopatological shape of the left coronary artery by means the centerlines of this vessel. The proposal is based on a sequential design which involves image enhancement, identification of all the types of vascular points belonging to the vascular system, construction of the coronary tree and tracking of the centerlines along the rotational angiography sequence. Some results obtained after applying this method to monoplane rotational X-ray image sequences are presented.

Keywords: Cardiac imaging, rotational angiography, left coronary artery, diffusion enhancement, optical flow.

1. INTRODUCTION

Coronary angiography has been used for assessing coronary arterial obstructions responsible for the morbidity and mortality caused by ischemic heart disease.¹ The morphology of the coronary arterial tree can be visualized in great detail by means of X-rays coronary angiography images.² Coronary assessment by means a X-ray conventional mono-plane angiography system requires multiple acquisitions at several viewing angles, and multiple injections of contrast product for defining the anatomy of the explored artery.

The estimation of artery stenosis grade from bidimensional (2-D) angiography projections, leading in some cases to the underestimation of the obstruction size because the shortening and overlapping of the cardiac structures evidenced in the projections introduce substantial error. In addition, the coronary obstructions do not have a circular luminal cross section, in consequence, lesions are only visible from certain views. Nonetheless, multiple angiography projections (a minimum of two) are required for major coronary arteries studies.³

The X-ray systems based on biplane angiography technology allow to acquire two orthogonal angiographies planes simultaneously with a single injection of contrast.⁴ Therefore, the angiography explorations using a biplane system in comparison with a single-plane system are becoming faster, the contrast load is significantly reduced, however, the biplane angiography systems deliver a significantly greater radiation dose.^{5,6} The technique is useful for patients with need for reduced contrast load as patients with renal failure and the pediatric population.⁷

Further author information: (Send correspondence to Gerardo Chacón.)

Gerardo Chacón: E-mail: j.chacon@unisimonbolivar.edu.co

Rotational angiography (RA) systems allow to acquire a sequence of images while the imaging gantry rotates continuously around the patient. The acquisition is rather fast, so the complete angiography sequence can be obtained within a single injection of contrast agent. As a result, the RA provides a complete range of projections, giving an excellent mental three-dimensional (3-D) representation of vascular structures, using less contrast agent than one single-angle angiogram sequence. This angiography technique was proposed around 1972.⁸

The clinical use of X-ray rotational angiography has been reported since 1983.⁹ Rotational digital subtraction angiography was reported in 1989¹⁰ and the 3-D reconstruction of RA sequences has been reported since 1997.¹¹ Although the three-dimensional rotational angiography has mainly been used in neuroradiology,¹² this technique is now used in cardiac applications for the analysis of coronary vessels, quantitative coronary angiography and the realization of interventional procedures.¹³⁻¹⁵

Some important works developed for assessing coronary heart disease from multiple projections of X-ray angiography have been reported. A system for coronary artery motion estimation in digital subtraction biplane angiography is reported in order to define and describe the motion features.¹⁶ The 3-D vessels reconstruction used to extract the dynamic features is performed from the main left coronary artery centerlines and then the motion features are evaluated along the sequence. The obtained results are consistent with artery dynamic.

An approach to coronary space-time reconstruction using RA is also reported.¹⁷ The coronary tree is reconstructed using arteries centerlines extracted from projections at the same instant of the cardiac cycle. Static 3-D reconstruction and a motion model are fused for correcting respiratory motion. The reconstructed centerlines and the respiratory motion compensation model are used to estimate the global motion. This research demonstrates the feasibility of the 3-D quantitative coronary analysis from angiography projections.

Three-dimensional LV reconstruction from RA projections is also a problem of interest. Kehl et al.¹⁸ have proposed a method for LV reconstruction from biplane RA sequences. The method is based on a backprojection method used in computerized tomography to reconstruct the LV cavity from rotational projections acquired during the same cardiac phase. The method works directly in 3-D space and does not require a segmentation stage. However, clinical validation and quantitative results are not provided.

In this paper, the enhancement and extraction of the left coronary artery tree from a non-subtracted RA is considered. The overall aim of this project is modeling (2-D + time) artery behavior by extracting the centerlines of the artery from the X-ray angiography projections. The proposed computational approach is fully automatic and it is based on a thorough analysis of the image intensities associated with left coronary artery on a local neighborhood in a complete sequence of rotational angiography projections.

2. METHOD

2.1 X-ray rotational angiography data

The AXIOM Artis Siemens rotational system is used to acquire the X-ray projections of left coronary artery. The acquisition protocol considers that the C-arm rotates from -30° right anterior oblique (RAO) angle to $+90^\circ$ left anterior oblique (LAO) angle to cover a range of 120° . The acquisition speed is 33.33 frames/s with a rotation speed of 40 degrees/s. Each rotational projection has a spatial resolution of 1024×1024 pixels and a pixel size of (0.1389×0.1389) mm. Each pixel is represented by 12 bits.

2.2 Image enhancement

The X-rays source of the AXIOM Artis system produces a not constant radiation during an acquisition. This variation produces changes in images brightness and in consequence, the background is not homogeneous for all images in the RA sequence. Figure 1 shows the histogram for an X-rays RA image sequence. The RA sequence, in this example, includes a total of 80 images. From the Figure the brightness variations in the sequence can be basically observed because there are projections containing more higher frequency information than others. Moreover, the distribution of the histogram between rotational projections is different.

An additional problem in rotational angiography is the fact that logarithmic subtraction techniques cannot be readily applied. The difficulty is related to the lack of synchronization between the acquisition of the mask

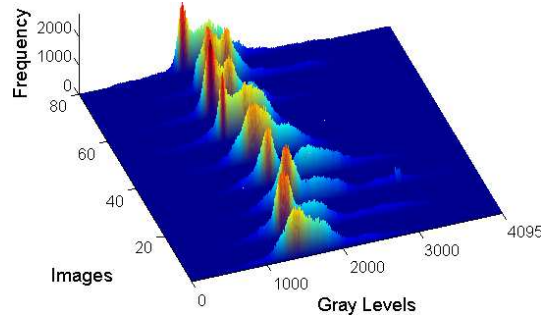


Figure 1. Rotational images histogram.

and the contrasted sequence. This synchronization is necessary for performing an accurate subtraction of images during the cardiac cycle.

An image smoothing approach is required to improve the left coronary artery information with respect to non-homogeneous background. The anisotropic diffusion filter is used for improving the vessel information, attenuating noise and reducing of the image artifacts impact. This filtering method is based on transforming the image to a function of its derivatives in a higher dimensional space. This higher dimensional function represents the heat diffusion equation solution 1.

$$\frac{dI(x, y; t)}{dt} = \nabla \cdot C(x, y) \nabla I(x, y; t) \quad (1)$$

with the initial state $I(x, y; 0) = \text{original image}$, $(x, y) \in \mathbf{R}^2$, t denotes time, and C represents the conductance.

Anisotropic diffusion methods are formulated for attenuating noise (or information non-desired) while preserving specific features in the images.¹⁹ The standard isotropic diffusion methods, like the Gaussian filter, are used to blur borders between the object and background while allowing changes in position of edges present in the image.²⁰ In contrast, the anisotropic diffusion methods are formulated to preserve edges. Anisotropic diffusion methods can be regarded as tools to obtain multi-resolution descriptions of images.²¹

2.3 Identification of centerlines points

The proposed computational approach considers the analysis of certain regions of the images instead of the total analysis of them, since the computational cost that represents any type of analysis on the whole image is high due to its size. For this purpose, it is proposed to analyze a series of profiles selected and extracted dynamically from the initial angiography projection of the rotational sequence processed by the anisotropic diffusion filter. Each profile represents a set of intensities of the image projection associated with pixels located along a horizontal line segment whose size is the width of the filtered image.

The angiography projection is split into three regions. The idea is that there is a greater number of profiles in the region located in the upper part of the image while in the other two regions the number of profiles is smaller. The 50% of the total profiles are located in the region of the upper part of the image, 30% in the second region and 20% of the total profiles in the last region. The Figure 2 shows the profiles distributed according to established criteria.

For each selected profile, a gradient-based difference operator defined as the magnitude of difference between two values of the intensities of current profile in an established spatial window, (equation 2).

$$\nabla_{ip} = |ip(i) - ip(i + \omega)| \quad , \quad (2)$$

where $ip(i)$ is a gray value in the current profile, n is the size of the profile and ω is the width of the window.

From the new profile obtained by applying the gradient-based difference operator, the mean square deviation is determined. This statistic represents the dispersion of the intensities of the new profile (∇ip) with respect its average value, according to equation (3).

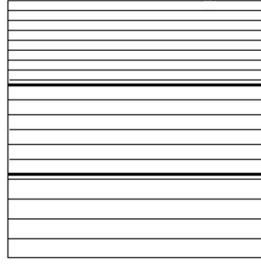


Figure 2. A distribution of the profiles.

$$\overline{std^2} = \frac{1}{n} \sum_{i=1}^n |\nabla ip(i) - \overline{\nabla ip}| \quad , \quad (3)$$

where $\overline{\nabla ip}$ is the mean of intensities in the profile and n the profile size.

The mean square deviation is considered a threshold value, used to define the pixel on the profile processed with the gradient-based difference operator in which an edge of an artery is verified. Due to the shape of the vessels in the angiographies projection, each candidate can be defined by two edges on the profile. The first edge of a candidate of an artery is checked in the pixel where the variation of the intensity of the profile processed with gradient-based difference operator changes from greater to less than the threshold. While the second edge is identified in the pixel with an intensity that exceeds the pre-established threshold. All structures verified with this procedure are considered candidates for arteries except those with thickness greater than 6 mm (45 pixels).

Since the coronary arteries have a certain maximum thickness (≤ 6 mm), those structures that do not meet this criterion are processed as follows: the segment greater than 6 mm is divided into 4 subsegments and then three vertical profiles, with a size of 4 times the maximum thickness of an artery, are established. After, these vertical profiles are analyzed with the gradient operator and the criteria based on the mean square deviation.

In this stage, in which the possible points belonging to the edges of coronary arteries have already been obtained in the first projection, and then the points of the centerline of the artery is established as the midpoint of the edge points, it is necessary to perform a debugging in order to discard points that are part of the background. To achieve this, a criterion based on a threshold is applied. For each of the three regions in which the filtered image has been divided, the mean is calculated and then considered as the threshold value. It is analyzed if the gray value of the current point is lower than the threshold of the region in which the point is located, if this is fulfilled, the point is discarded as a point on the centerline of the artery.

A method proposed to capture the common properties shared by polar neighborhood intensity profiles for all the types of vascular points belonging to the vascular system²² is used in this research for validating that the candidates points really belong to the centerline of the artery. Moreover, the method is used to identify the vessel end points, the points around the vessel center, the branching points and the crossing points.

2.4 Left coronary tree construction

The left coronary tree is built from the concatenation of the previously detected branches. The procedure for branch detection begins with the location of the branching points, basically because the dichotomous property of the arteries establishes that an artery always divides into two branches. Therefore, it is considered that for each branching point there must be three branches as shown in the Figure 3 and each branch has a series of points associated.

Two points belonging to the same branch must have a similar slope to it must meet the condition (4), in which m_0 is the slope of the line between the last two points of each branch and m is the slope between the last point of the branch and the point that will be analyzed.

$$m_0 - \frac{\pi}{6} \leq m \leq m_0 + \frac{\pi}{6} \quad . \quad (4)$$

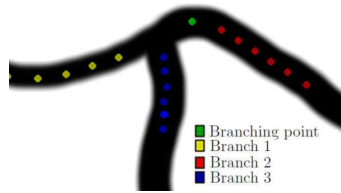


Figure 3. Branches at the branching point.

For each of the branches in a branching point, a search of nearby points previously classified as points around the vessel center is performed. Once the respective branches are obtained for each branching point, the distances between points around the vessel center and the slopes of the line that would join them are compared with the aim of joining such points. The process of joining the points starts from the end point of a branch to the end point of each of the other bifurcations as shown in Figure 4. As expected, in some cases the process ends when a vessel end point is found.

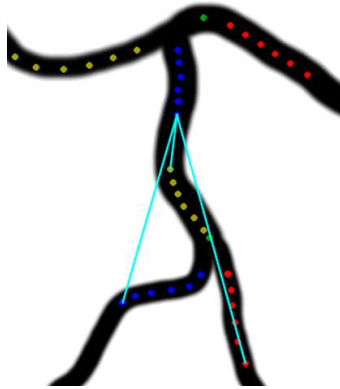


Figure 4. Comparison of distances between ends of branches.

Finally, when all the branches joined, the left coronary tree is represented by the set of lines defined in the process of joining the points. The morphology of the left coronary artery presents certain curved regions which are not modeled correctly with the use of straight lines. In this sense, a b-spline procedure²³ is used to estimate a better model of the vessel tree from the points that defines the straight lines.

2.5 Vessel centerline tracking

The algorithm proposed for the estimation of the optical flow that takes into account the deviations both for the assumption of the brightness invariability and for the softness of the motion field,²⁴ and subsequently modified by incorporating a heuristic scheme based on weighted median filtering,²⁵ is used to track the points of the left coronary centerline in the rotational angiography projections sequence.

3. RESULTS

The left coronary angiograms acquired using the rotational mode is used to evaluate the proposed method. The enhancement procedure described in section 2.2 is applied to the rotational projections sequence. The diffusion filtering procedure is implanted considering a constant conductance (C). Several values of conductance are applied in equation 1 to obtain a solution to the heat equation. A value of 2.5 is empirically selected. The Insight ToolKit (ITK) is used for implementing the anisotropic diffusion based enhancement. The ITK is a toolkit which includes several image processing algorithms. These tools have been widely used for teaching and development of medical image processing systems.²⁶ Results are shown in Figure 5. It can be observed that the background looks more homogeneous while associated arteries information is enhanced. Additionally, in the profiles shown the noise reduction and vessel information enhancement can be observed.

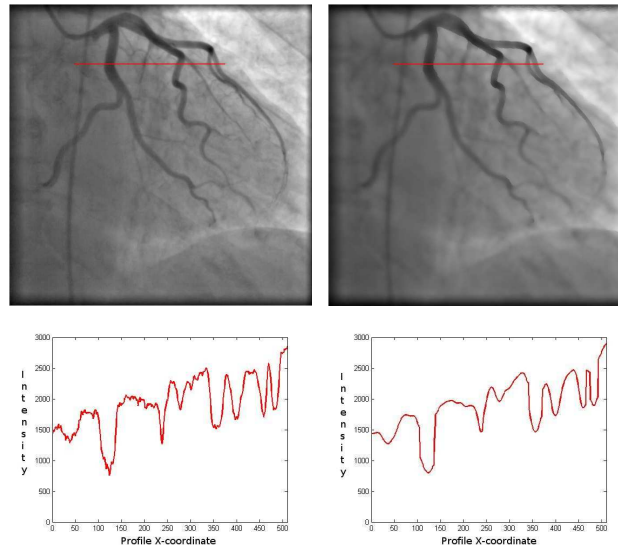


Figure 5. Left coronary images. Original images in the first column and enhancement images in the second column. Original and smoothed image profiles.

Figure 6 shows the three regions in which the angiographic projection is split, and the horizontal lines that will define the image profiles to be analyzed.

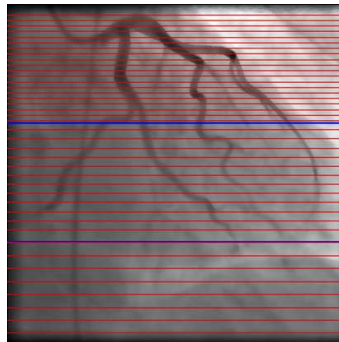


Figure 6. Profiles in the regions of the angiographic projection.

The procedure to analyze the selected profiles of the angiographic projection is graphically shown in the Figure 7. This Figure shown, a region-of-interest that contains one profile, the information of gray level intensities, and the result obtained when applying the gradient-based difference operator to image intensities in this profile. For the gradient-based difference operator, ω is set to 8 because the pixel size is 0.1389×0.1389 mm in the rotational angiography projections and this value is considered as the minimum diameter of a coronary artery (~ 1 mm).

Figure 8.a shows all the points associated with the artery edges located with the profile analysis procedure, and Figure 8.b shows the final edge points after debugging performed to discard points that are part of the background, the points discarded are tagged with black.

The stages of the method to identify the types of vessel points is graphically described in Figure 9. In the first column of the Figure 9 the radial profiles with center in the point to analyze are shown for the vessel end points, the points around the vessel center, the branching points and the crossing points. The information associated with the radial profiles is represented in rectangular coordinates as shown in the second column of Figure 9. Each column of the rectangular image is resampled every 3 positions. The gray values obtained from this resampling are used to estimate the gray level behavior in the polar neighborhood (third column of Figure 9). In the fourth column of Figure 9, the identified point is tagged by a green circle.

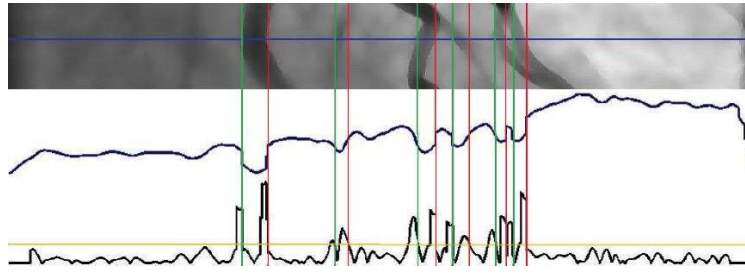
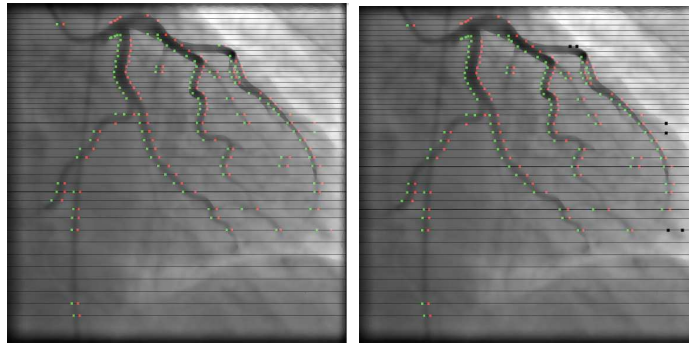


Figure 7. Analysis of the image profiles.



(a)

(b)

Figure 8. Estimated edges of the left coronary artery.

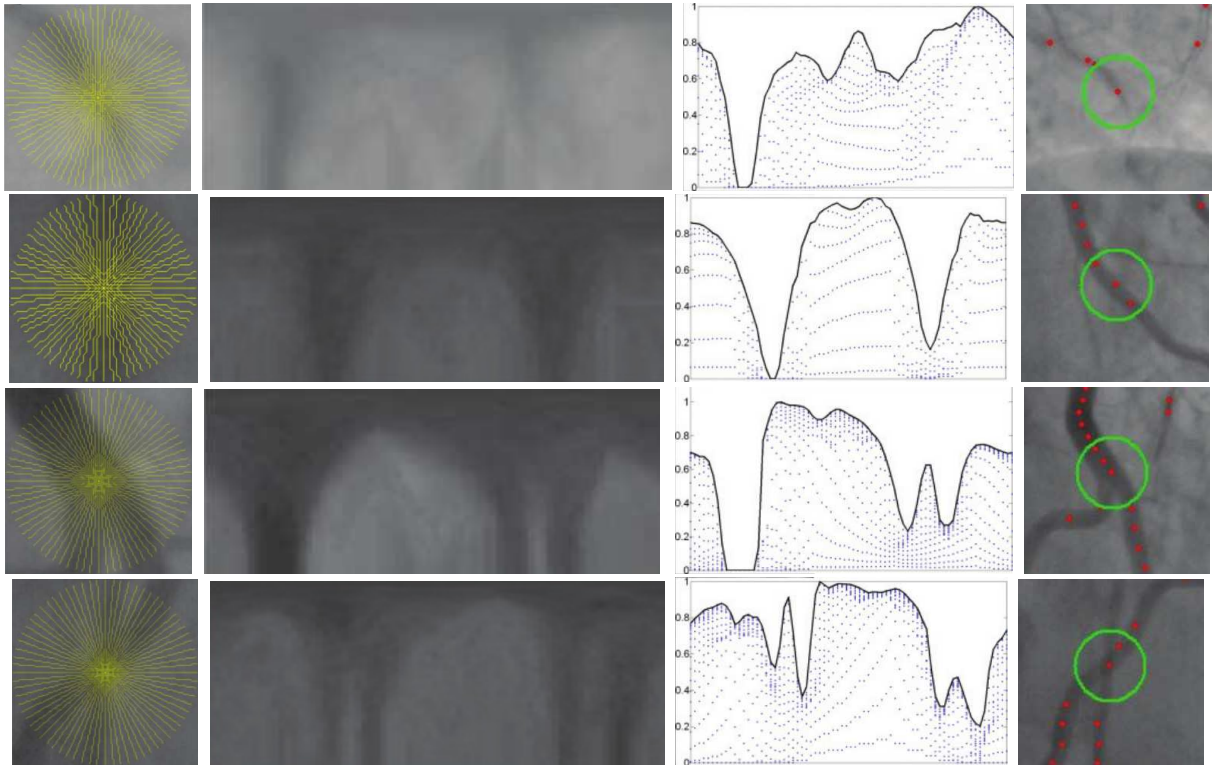


Figure 9. Types of vessel points.

Validation of the artery points identification method is performed by quantifying the absolute error (in mm) between the estimated points location with respect to the points located by a cardiologist. The average error obtained (mean \pm standard deviation) for the points in the initial angiography projection is 1.94 ± 1.1 mm, with

a maximum value of 3.27 mm and a minimum value of 0.93 mm. The maximum error represented 24 pixels.

The left coronary tree represented by the set of straight lines is shown in Figure 10.a, meanwhile the left coronary tree represented by the set of b-spline curves is shown in Figure 10.b. The catheter is labeled as an isolated branch of the coronary tree.

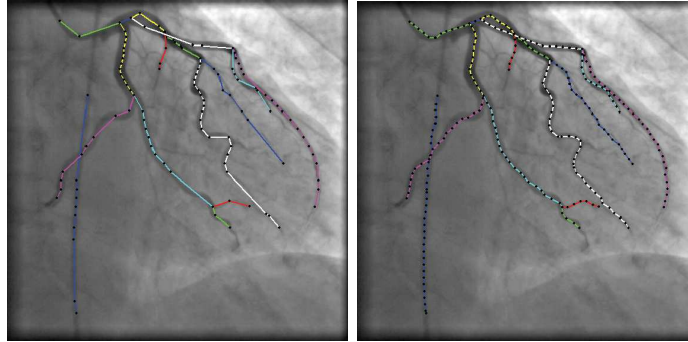


Figure 10. Left coronary tree built.

The application of the algorithm for the estimation of the optical flow at the points of the artery centerline, allows to track these points along to rotational angiography sequence. As can be seen from the Figure 11, the tracking of the centerlines points along the rotational sequence is lost, basically because the contrast agent injected into the coronary artery decreases as the sequence progresses. Additionally, the crossing of two branches of the artery during rotation also causes the follow-up to be lost.

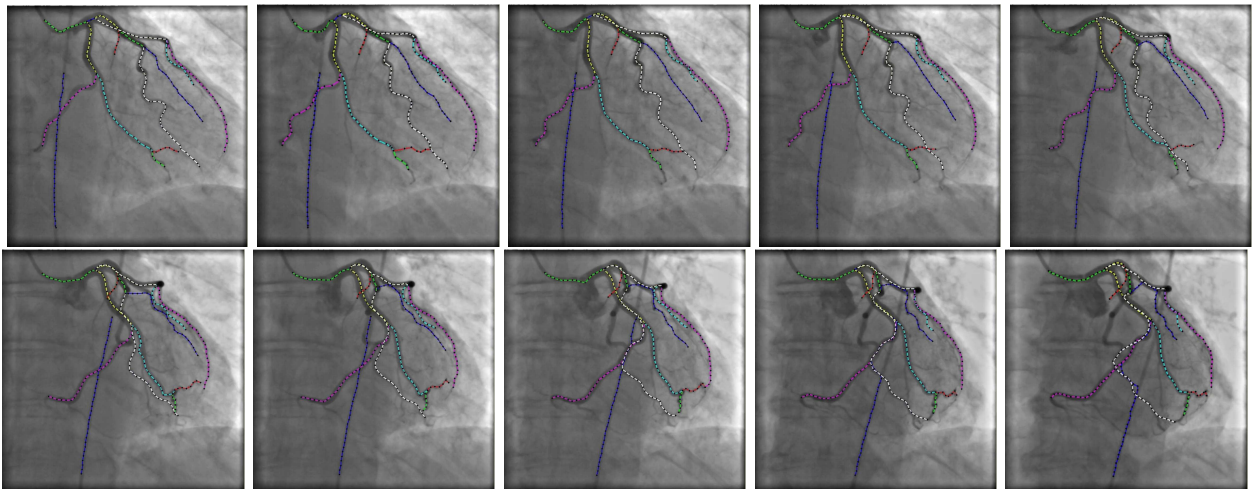


Figure 11. Results of the tracking process of the left coronary artery centerlines.

4. CONCLUSION

An automatic computational approach for extracting the left coronary artery centerlines has been presented. This approach has been applied to un-subtracted angiograms of left coronary vessel acquired on a RA equipment. The technique requires only the minimum size of the coronary vessels as prior knowledge. The approach identifies successfully the vessel end points, the points around the vessel center, the branching points and the crossing points.

The effectiveness of the centerlines extraction method relies on the homogeneity obtained by using an anisotropic diffusion method. The anisotropic diffusion filtering enables attenuation of image noise. Nevertheless, the changes in image brightness remain along the rotational sequences. Consequently, the non-homogenous

structures in the projections could induce losing track of the centerlines points along the sequence. This problem could be solved by applying an adaptive diffusion filtering technique. The idea would be to consider a conductance parameter estimated as a function of the space and time instant.

The method should incorporate more complex motion analysis techniques in order to improve the tracking process of the left coronary artery centerlines on the rotational sequence.

As a further research, the application of this approach for performing the detection of centerlines of right coronary artery in images acquired according to the rotational angiography mode is proposed. A more complete validation is also necessary, including control subjects as well as cardiac patients. The validation stage could also include a comparison of estimated parameters describing the cardiac motion.

ACKNOWLEDGMENTS

Authors would like to thank the Universidad Simón Bolívar, Colombia, and Investigation Dean's Office of Universidad Nacional Experimental del Táchira, Venezuela for their support to this research. Authors would also like to thank Hervé Le Breton and Dominique Boulmier from the Centre Cardio-Pneumologique in Rennes, France for providing the human angiography database. This work was supported by the Universidad Simón Bolívar, Colombia (grant: C2011520216).

REFERENCES

- [1] Pantos, I., Efstathopoulos, E. P., and Katritsis, D. G., "Two and three-dimensional quantitative coronary angiography," *Cardiology Clinics* **27**(3), 491–502 (2009).
- [2] Windecker, S. and Meier, B., "X-ray coronary angiography," in [*Pan Vascular Medicine: Integrated Clinical Management*], Lanzer, P. and Topol, E. J., eds., 602–635, Springer, Berlin, Heidelberg (2002).
- [3] Di Mario, C. and Sutaria, N., "Coronary angiography in the angioplasty era: projections with a meaning," *Heart* **91**(7), 968–976 (2005).
- [4] Robb, G. and Steinberg, I., "Visualization of the chambers of the heart, the pulmonary circulation, and the great blood vessels in man: A practical method," *American Journal of Roentgenology* **41**(1), 1–17 (1939).
- [5] Onnasch, D., Schmiel, F.-K., and Kramer, H.-H., "Problems in quantitative evaluations of biplane x-ray angiocardiograms," *International Congress Series* **1230**, 1010–1016 (2001).
- [6] Sadick, V., Reed, W., Collins, L., Sadick, N., Heard, R., and Robinson, J., "Impact of biplane versus single-plane imaging on radiation dose, contrast load and procedural time in coronary angioplasty," *The British Journal of Radiology* **83**(989), 379–394 (2010).
- [7] Kern, M., Sorajja, P., and Lim, M., [*Cardiac Catheterization Handbook E-Book*], Elsevier Health Sciences (2015).
- [8] Cornelis, G., Bellet, A., van Eygen, B., Roisin, P., and Libon, E., "Rotational multiple sequence roentgenography of intracranial aneurysms," *Acta Radiologica: Diagnosis* **13**(1), 74–76 (1972).
- [9] Thron, A. and Voigt, K., "Rotational cerebral angiography: procedure and value," *American Journal of Neuroradiology* **4**(3), 289–291 (1983).
- [10] Schumacher, M., Kutluk, K., and Ott, D., "Digital rotational radiography in neuroradiology," *American Journal of Neuroradiology* **10**(3), 644–649 (1989).
- [11] Carsin, M., Chabert, E., Croci, S., Romeas, R., and Scarabin, J.-M., "[The role of 3-dimensional reconstructions in the angiographic evaluation of cerebral vascular malformations: 3D morphometry]," *Journal of Neuroradiology* **24**(2), 137–140 (1997). in French.
- [12] Anxionnat, R., Bracard, S., Macho, J., Costa, E. D., Vaillant, R., Troussset, L. L. Y., Romeas, R., and Picard, L., "3D angiography clinical interest. First applications in interventional neuroradiology," *Journal of Neuroradiology* **25**(4), 251–262 (1998).
- [13] Raman, S., Morford, R., Neff, M., Attar, T., Kukielka, G., Magorien, R., and Bush, C., "Rotational X-ray coronary angiography," *Catheterization Cardiovascular Interventions* **63**(2), 201–207 (2004).
- [14] Green, N. E., Chen, S.-Y., Messenger, J. C., Groves, B. M., and Carroll, J. D., "Three-dimensional vascular angiography," *Current Problems in Cardiology* **29**(3), 104–142 (2004).
- [15] Klein, A. J. and Garcia, J. A., "Rotational coronary angiography," *Cardiology Clinics* **27**(3), 395–405 (2009).

- [16] Puentes, J., Roux, C., Garreau, M., and Coatrieux, J., “Dynamic feature extraction of coronary artery motion using DSA image sequences,” *IEEE Transactions on Medical Imaging* **17**(6), 857–871 (1998).
- [17] Blondel, C., Malandain, G., Vaillant, R., and Ayache, N., “Reconstruction of coronary arteries from a single rotational X-ray projection sequence,” *IEEE Transaction on Medical Imaging* **25**(5), 653–663 (2006).
- [18] Kelh, H., Jäger, J., Papazis, N., Dimitrelos, D., Gehrmann, J., Kassenböhmer, R., Vogt, J., and Sakas, G., “3D heart modeling from biplane rotational angiocardiographic X-ray sequences,” *Computers & Graphics* **24**(5), 731–739 (2000).
- [19] Cañero, C. and Radeva, P., “Vesselness enhancement diffusion,” *Pattern Recognition Letters* **24**(16), 3141–3151 (2003).
- [20] Meijering, H., *Image Enhancement in Digital X-Ray Angiography*, PhD thesis, Utrecht University (Oct 2000).
- [21] Frangi, A., Niessen, W., Vincken, K., and Viergever, M., “Multiscale vessel enhancement filtering,” in [*Proceedings MICCAI*], LNCS, 130–137 (1998).
- [22] Qian, X., Brennan, M. P., Dione, D. P., Dobrucki, W. L., Jackowski, M. P., Breuer, C. K., Sinusas, A. J., and Papademetris, X., “A non-parametric vessel detection method for complex vascular structures,” *Medical Image Analysis* **13**(1), 49–61 (2009).
- [23] Barsky, B., [*Computer graphics and geometric modeling using Beta-splines*], Springer-Verlag (1998).
- [24] Black, M. J. and Anandan, P., “The robust estimation of multiple motions: Parametric and piecewise-smooth flow fields,” *Computer Vision and Image Understanding* **63**(1), 75–104 (1996).
- [25] Sun, D., Roth, S., and Black, M. J., “Secrets of optical flow estimation and their principles,” in [*IEEE Conf. on Computer Vision and Pattern Recognition (CVPR)*], 2432–2439, IEEE (June 2010).
- [26] Shelton, D., Stetten, G., Aylward, S., Ibez, L., Cois, A., and Stewart, C., “Teaching medical image analysis with the insight toolkit,” *Medical Image Analysis* **9**(6), 605–611 (2005).